CO Adsorption and Reaction on Clean and Oxygen-Covered Au(211) Surfaces

Jooho Kim,[†] Enrique Samano,[‡] and Bruce E. Koel*[,†]

Department of Chemistry, Lehigh University, Bethlehem, Pennsylvania 18015-3172, and CCMC-UNAM, Ensenada, B.C., Mexico

Received: March 17, 2006; In Final Form: June 30, 2006

We have used primarily temperature-programmed desorption (TPD) and infrared reflection−absorption spectroscopy (IRAS) to investigate CO adsorption on a Au(211) stepped single-crystal surface. The Au(211) surface can be described as a step-terrace structure consisting of three-atom-wide terraces of (111) orientation and a monatomic step with a (100) orientation, or 3(111) × (100) in microfacet notation. CO was only weakly adsorbed but was more strongly bound at step sites (12 kcal mol^{-1}) than at terrace sites (6.5−9 kcal mol^{-1}). The sticking coefficient of CO on the Au(211) surface was also higher (∼5×) during occupation of step sites compared to populating terrace sites at higher coverages. The ν_{CO} stretching band energy in IRAS spectra indicated that CO was adsorbed at atop sites at all coverages and conditions. A small red shift of ν_{CO} from 2126 to 2112 cm^{-1} occurred with increasing CO coverage on the surface. We conclude that the presence of these particular step sites at the Au(211) surface imparts stronger CO bonding and a higher reactivity than on the flat Au(111) surface, but these changes are not remarkable compared to chemistry on other more reactive crystal planes or other stepped Au surfaces. Thus, it is unlikely that the presence or absence of this particular crystal plane *alone* at the surface of supported Au nanoparticles has much to do with the remarkable properties of highly active Au catalysts.

Introduction

Gold has often been referred to as the noblest metal. The result of this low reactivity is that historically, while Au-based catalysts have been reported as useful for some reactions, Au catalysts were usually considered to be much less active for most reactions than catalysts incorporating Pt or other group VIII transition metals, and even the other group IB metals Ag or Cu. Gold has attracted renewed attention due to reports of high catalytic activity for H_2 and CO oxidation on nanosized gold particles supported on reducible metal oxides at low temperature (even at 200 K).[1−17] Haruta and co-workers[1−3] first reported this surprisingly high catalytic activity for nominally 2 nm gold particles supported on TiO_2, α-Fe_2O_3, Co_3O_4, and NiO. Au/TiO_2 catalysts were of particular interest because both Au and TiO_2, independently, adsorb CO and O_2 only weakly.

In fundamental studies related to such oxidation catalysis, several surface science studies of O_2 adsorption on gold have been carried out both under UHV conditions and at high pressures.[18−20] No study has reported any significant O_2 activation or dissociation to form oxygen adatoms on any gold substrate, including stepped or polycrystalline surfaces between 200 and 500 K. CO adsorbs weakly on the Au(100) surface at 82 K[21] and does not adsorb on Au(111) at 85 K under UHV conditions.[22] CO adsorption does not occur on clean or oxygen-covered Au(110) surfaces at 125 K indicating that the CO adsorption energy is less than 8 kcal mol^{-1}.[19] CO adsorbs on Au(110) at 50 K with an adsorption energy that is intermediate between that on Cu(100)-c(2 × 2) and Ag(110) surfaces.[23] Recently, Gottfried et al. reported CO adsorption on Au(110)-(1 × 2) at 28 K with two CO desorption states in temperature-programmed desorption (TPD) at T_p = 67 and 145 K with E_{ads} = 4.4 and 9.0 kcal mol^{-1}, respectively, from the monolayer.[24]

The lower coordination number of metal atoms at step sites usually imparts additional reactivity at those sites. CO adsorption has been investigated on several stepped gold surfaces. CO adsorbed weakly on the Au(332) surface at 92 K with a saturation coverage reported to be 0.17 ML.[25,26] A CO TPD peak at 185 K was attributed to CO bound at step sites, and a peak at 140 K was assigned to CO bound at terrace sites. From the infrared reflection−absorption spectroscopy (IRAS) spectra, the ν_{CO} stretching mode of CO bound at step sites occurred at 2125 cm^{-1}, and ν_{CO} of CO on terraces was at 2113 cm^{-1}. On a 1.1 ML gold-covered Pt(335) surface, CO desorbed in TPD measurements at 105 K with two small shoulders at 190 and 220 K.[27] However, the authors suggested that these desorption states might be caused by the influence of the underlying Pt or by defects in the film. On partly or fully Au-covered Pd(111) at 110 K, CO adsorption formed linearly bonded CO molecules at Au atoms in the upper terrace at the edge of Au islands or steps with a stronger Au−CO bond than that at typical Au terrace sites.[28,29] No adsorbed CO was found on the Au terrace sites at 110 K.

Thus, surfaces of bulk Au samples do not appear to chemisorb either O_2 or CO (although physisorbed species might be formed under some conditions) and are not catalytically active for CO oxidation from O_2 + CO. Many theories have been suggested to explain the high catalytic activity of nanosized gold particles for CO oxidation. For example, Haruta[30] proposed a reaction mechanism for CO oxidation over Au/TiO_2 catalysts in which it was suggested that CO adsorbed on the surface of the Au particles and O_2 adsorbed on the surfaces of the TiO_2 support. CO oxidation then proceeds at the perimeter interfaces at 200−300 K and forms carbonate species. Boccuzzi et al.[31] also

* Corresponding author. Phone: +1-(610) 758-5650. Fax: +1-(610) 758-6555. E-mail: brk205@lehigh.edu.
[†] Lehigh University.
[‡] CCMC-UNAM.

10.1021/jp061685d CCC: $33.50
Published on Web 08/17/2006

proposed that the first step in the CO oxidation reaction at room temperature was the adsorption of mobile O_2 species at defect sites on the oxide support followed by dissociation at the interface between Au step sites and the oxide. Then, adsorbed oxygen species "spill over" to the Au particles where they react with adsorbed CO. In reports from Goodman and co-workers[32,33] in which they investigated more clearly the dependence of CO oxidation activity on the Au cluster size on planar TiO_2 supports, they proposed that the structure sensitivity could be related to a quantum size effect with respect to the thickness of the gold islands. They found that Au islands that were two atomic layers thick were the most effective for catalyzing CO oxidation and possessed unusual electronic properties.

Insights from theoretical calculations are also available. Landman and co-workers[34,35] calculated CO oxidation on the Au anion dimer, Au_2^-, and determined that $Au_2CO_3^-$ was a key metastable intermediate to produce CO_2 with an activation barrier of 12 kcal mol^{-1}. Mavrikakis et al.[36] explored the reactivity of gold on the basis of self-consistent density functional theory (DFT) calculations of O_2 and CO adsorption on flat Au slabs with 1−6 layers and on Au(211) stepped slabs. The reactivity of Au(111) slabs had little variation except for the one-layer slab, which was less reactive than all of the others. CO adsorbed stronger on step sites than (111) terrace sites. The O_2 dissociative adsorption activation energy on the Au(211) stepped surface was nearly thermoneutral, while it was a positive value on the Au(111) surface. It was proposed that O_2 might dissociate on the step edges on Au(211). They also proposed that the unusually high catalytic activity of gold particles on supports might be partly due to high step density and strain effects from lattice mismatch of Au particles on supports. Liu et al.[37] reported DFT calculations of CO adsorption energies on the Au(111), Au(211), and Au(221) surfaces to be 4.0, 24.9, and 23.7 kcal mol^{-1}, respectively. These CO adsorption energies on the Au stepped surfaces seem to be somewhat too high considering that the CO desorption energy on Au(332) is less than 13 kcal mol^{-1}.[26]

To provide additional data on the reactivity of Au(211) surfaces, and also benchmark such theoretical calculations, we report here on TPD and IRAS investigations of CO adsorption on a Au(211) single-crystal surface.

Experimental Methods

Experiments were conducted in a two-level stainless steel UHV chamber that has been described previously.[38] The system had a base pressure of 2×10^{-10} torr. The lower level was equipped for AES, TPD, and LEED studies, and an attached batch reactor on the upper level had facilities for Ar^+-ion sputtering, IRAS measurements, and high-pressure kinetics studies.

The Au(211) crystal (Metal Crystal & Oxides, LTD, diam 10 mm × 2 mm thick) was mounted using two 0.015 in. diameter W wires attached to two 0.126 in. diameter Ta rods that were pressed into a liquid-nitrogen-cooled Cu block. The crystal could be heated resistively to 1100 K and cooled to 85 K as monitored by a chromel−alumel thermocouple pressed firmly (using Au foil) into a small hole in the side of the crystal. The crystal was cleaned by repeated Ar^+-ion sputtering (500 eV, 2 μA) for 10 min with the sample at 300 K and annealing at 985 K for 10 min in UHV. This procedure was repeated until the carbon peak in AES (E_p = 3 keV) did not decrease any more (θ_c = 0.02 ML). After this, the sample was treated by exposure to 10^{-5} torr of O_2 at 873 K for 5 min and flashed to 985 K for 1 min to eliminate any trace of carbon on the surface. After this initial extensive cleaning procedure, exposing the sample to oxygen ($P_{O_2} = 10^{-5}$ torr) at 873 K for 5 min and flashing the surface to 985 K for 1 min was sufficient to remove any small carbon residue that accumulated at the surface.

High-purity CO (Matheson Gas Products, UHP grade, 99.9% purity) was used in the UHV chamber without further purification. Ozone used for dosing in UHV was prepared in our laboratory using a commercial ozone generator as described elsewhere.[39]

TPD experiments were performed with the crystal in line-of-sight of the ionizer of the quadrupole mass spectrometer (QMS) and a heating rate of 3 K s^{-1}. QMS signals at m/e = 18, 28, 32, and 44 were monitored simultaneously. The mass spectrometer was shielded, and the sample was placed close (∼2 mm) to the entrance aperture of the shield in order to discriminate against desorption not coming from the crystal front face. IRAS was performed by using a Mattson Infinity 60MI spectrometer operated at 4 cm^{-1} resolution and accumulating 1000 scans.

CO was leaked into the UHV chamber through a Varian leak valve with an attached stainless steel tube and microcapillary array to achieve a directed gas beam and exposure of gas on the sample front face without prior reaction with the chamber walls. CO exposures are reported herein after calculating the exposure by using the background pressure measured by the ion gauge and then multiplying this value by a factor of 5 to account for the doser enhancement of the gas exposure over that of the random flux in the chamber. This enhancement factor was directly measured at the beginning of these experiments by comparing the CO TPD area resulting from small CO doses from the background gas with those results obtained by using the doser. Ozone was dosed similarly onto the Au(211) surface via a second doser, but reported ozone exposures are for relative comparisons only, since some ozone decomposition occurs in the gas lines and leak valve and the increased pressure in the chamber that is measured is due partially to O_2.

Results and Discussion

The Au(211) surface is described as 3(111) × (100) in microfacet notation, i.e., a step-terrace structure consisting of three-atom-wide terraces of (111) orientation and a monatomic step with a (100) orientation. Structural details and our LEED characterization of the Au(211) surface can be found elsewhere.[20]

CO Adsorption on Au(211). Temperature-programmed desorption (TPD) experiments were performed following CO exposures from 0.0025 to 50 langmuir (L) on the Au(211) surface at 85 K. As shown in Figure 1, TPD curves exhibited a peak at 190 K (α) and a broad feature from 100 to 150 K (β_1 = 150 K, β_2 = 127 K, and β_3 = 109 K). The α peak shifted from 197 to 190 K with increasing exposures. This peak was attributed to desorption of CO from step sites on the Au(211) surface. The CO desorption energy E_d for this peak was roughly estimated to be 12 kcal mol^{-1} by utilizing Redhead analysis assuming first-order desorption kinetics and a preexponential factor of 10^{13} s^{-1}. The broad feature at lower temperatures was attributed to CO desorption from terrace sites. The β_1 peak appeared initially at 150 K after 0.025 langmuir CO exposure. The β_2 and β_3 peaks at 127 and 109 K, respectively, were observed after 0.1 langmuir CO exposure. Values of E_d for CO desorption in these peaks were roughly estimated to be 6.5 kcal mol^{-1} (β_3), 8 kcal mol^{-1} (β_2), and 9 kcal mol^{-1} (β_1) by Redhead analysis as above.

An "uptake curve" can be constructed from the TPD data to obtain information on the CO adsorption kinetics. Such a curve

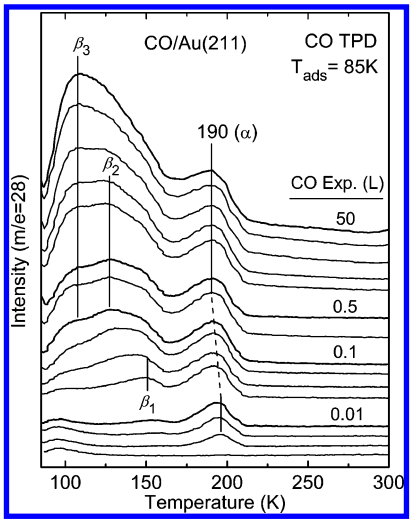

Figure 1. CO TPD curves obtained after dosing 0.0025−50 langmuir (L) CO on Au(211) at 85 K. Results are shown for CO exposures of 0, 0.0025, 0.005, 0.01, 0.025, 0.05, 0.75, 0.1, 0.25, 0.5, 2.5, 5, 10, 25, and 50 langmuir. Peaks are identified as $\alpha = 190$ K, $\beta_1 = 150$ K, $\beta_2 = 127$ K, and $\beta_3 = 109$ K. The bottom curve is for CO desorption from background accumulation only, with no CO dose given.

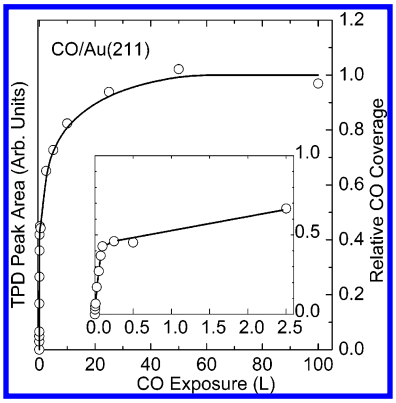

Figure 2. Uptake curve for CO adsorption on Au(211) at 85 K. This was constructed from the CO TPD peak areas from data presented in Figure 1. The inset shows CO uptake in the low-exposure regime (0−2.5 langmuir) on an expanded scale. CO adsorbs more efficiently below 0.1 langmuir exposure, and then the CO sticking coefficient decreases significantly.

is shown in Figure 2, in which the TPD peak areas obtained from the curves in Figure 1 are plotted as a function of the CO exposure used. Relative CO coverages calculated from the saturation coverage at 85 K are shown at the right axis. CO adsorption on the surface is initially very rapid with a constant sticking coefficient, which is given by the slope of the curve in this plot. Thus, CO adsorption occurs initially at step sites with high efficiency with non-Langmuirian adsorption kinetics via a precursor-mediated adsorption mechanism. Following saturation of these sites, additional CO adsorption occurs on the terrace sites with a lower adsorption energy and a reduced sticking coefficient that is 4.6 times smaller than onto the steps. The CO adsorption more nearly resembles Langmuirian adsorption kinetics at higher coverages.

Figure 3 shows data obtained to explore the influence of thermally induced restructuring or ordering of the CO monolayer on the CO TPD curves. These experiments were carried out by exposing 0.5 langmuir CO on Au(211) at 85 K, flashing the surface to a given higher temperature and recooling to 85 K, and then subsequently performing TPD measurements. CO associated with the terrace sites on Au(211) was removed by heating the sample to 160 K, and only CO bound at step sites

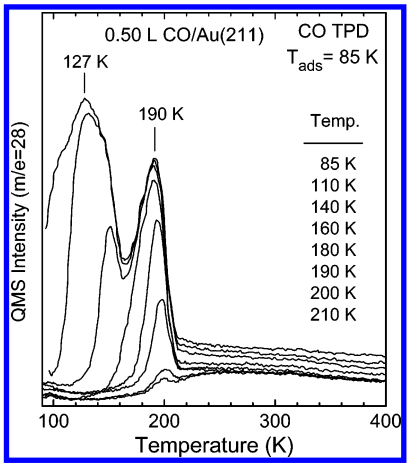

Figure 3. CO TPD curves obtained after dosing 0.5 langmuir (L) CO on Au(211) at 85 K and then preannealing to various temperatures. CO remains only at the Au(211) step sites after annealing to 160 K.

was left on the surface. The amount of CO left on Au(211) step sites at 160 K was estimated to be 14% of the saturation coverage formed by a 50 langmuir CO dose (the difficulty of clearly discriminating background effects in the TPD spectra from large doses causes uncertainty in this estimation, and that of the sticking coefficient at high coverage).

In previous studies reported by Ruggiero and Hollins,[25] CO desorption from a stepped Au(332) surface showed similar behavior. This surface can be described as 6(111) × (100) in microfacet notation indicating a step-terrace structure consisting of six-atom-wide terraces of (111) orientation and a monatomic step with a (100) orientation. CO desorbed in two peaks at 140 and 185 K in TPD after exposing CO on the surface at 92 K. The saturation coverage of CO on Au(332) at 92 K was reported as 0.17 ML using the measured dipolar-coupling shift in IR experiments. Results are also available for several related metal surfaces. CO TPD curves from a Cu(332) surface showed three CO desorption states in the experiments of Bönicke et al.[40] After comparing their results with CO TPD data on Cu(111) and Cu(110) surfaces, they suggested that the higher temperature peak was from step sites and the other was from terrace sites. On the stepped 6(111) × (100) and 6(111) × (111) Pt surfaces, a high-temperature TPD peak was assigned to CO desorption from step sites with $E_d = 33$ kcal mol^{-1}.[41] The value for CO adsorbed at terrace sites was $E_d = 24-27$ kcal mol^{-1}.

Figure 4 shows IRAS spectra of CO adsorbed on Au(211) at 85 K for increasing CO doses. Adsorbate spectra in IRAS were taken after CO was exposed on the surface at 85 K, and then the associated reference spectra were obtained after heating the sample to 700 K to desorb all CO from the surface. The value of ν_{CO} for CO adsorbed on Au(211) after the lowest exposure (0.005 langmuir) appeared at 2122 cm^{-1}, and this shifted to 2112 cm^{-1} after exposures larger than 0.25 langmuir. This value did not shift further with higher CO exposures.

In addition, IRAS was used to probe restructuring or ordering in the CO monolayer due to heating. Figure 5 shows IRAS spectra after 0.5 langmuir CO was exposed on Au(211) at 85 K and after the sample was flashed to successively higher temperatures of 110−200 K. These spectra were obtained after the sample had recooled to 85 K following each annealing step. Increasing the flash temperature caused the ν_{CO} peak to shift from 2112 cm^{-1} at 85 K to 2126 cm^{-1} at temperatures higher than 190 K where θ_{CO} was less than 3% of the saturation coverage.

Because the IRAS spectra showed a ν_{CO} band that was higher than 2100 cm^{-1} in all cases, CO can be considered to be bonded

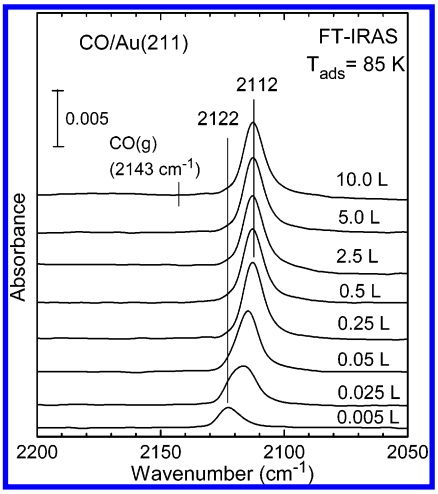

Figure 4. Vibrational spectra from IRAS obtained after dosing 0.005−10 langmuir CO on Au(211) at 85 K. The ν_{CO} mode of CO adsorbed on Au(211) after the lowest exposure (0.005 langmuir) occurs at 2122 cm^{-1}, and then it shifts to 2112 cm^{-1} with increasing exposure. The position of ν_{CO} (2143 cm^{-1}) for gas-phase CO is marked on the top spectrum for comparison.

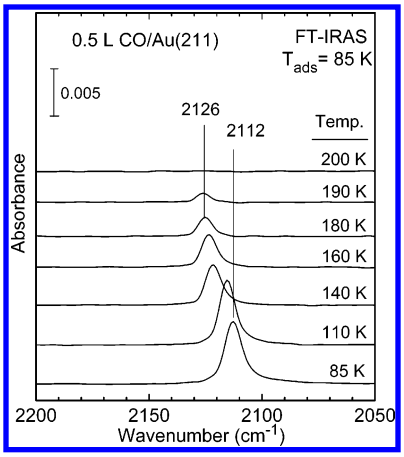

Figure 5. Companion IRAS spectra to Figure 3 that were obtained after dosing 0.5 langmuir CO on Au(211) at 85 K and then subsequently flashing the crystal to various temperatures in the range of 85−200 K. The spectra were taken after recooling the surface to 85 K. The ν_{CO} band appeared at 2112 cm^{-1} at 85 K and shifted to 2126 cm^{-1} after flashing to 190 K. Flashing above 200 K removes all CO from the surface.

at atop sites on the surface, regardless of whether adsorption is associated with terraces or steps. The red shift of ν_{CO} for adsorbed CO with increasing CO coverage on Au surfaces has been reported and explained previously by using two opposing effects: dipolar coupling and chemical shift. Dipolar coupling tends to increase ν_{CO}, while a chemical effect can shift the band either to lower or higher wavenumbers as θ_{CO} increases. Dumas et al.[42,43] investigated both effects on Au films by recording spectra from $^{12}CO/^{13}CO$ mixtures. Such an isotopic mixture allows dipolar-coupling shifts to be reduced in a controlled way, while leaving chemical shifts unchanged. They found that the total shift of −13 cm^{-1} (ν_{CO} = 2125 cm^{-1} at one-tenth of saturation coverage and ν_{CO} = 2112 cm^{-1} at saturation coverage) could be resolved into a dipolar-coupling shift of +17 cm^{-1} and a chemical shift of −30 cm^{-1}. France and Hollins[44] in studies of Au supported on silica using isotopic mixtures found that ν_{CO} shifted from 2129 cm^{-1} at a pressure of 0.001 torr CO to 2106 cm^{-1} at 760 torr CO. This red shift in ν_{CO} with increasing CO coverage was attributed to the combination of a small positive dipolar component and a larger negative chemical shift component. The red shift of ν_{CO} in our results with increasing θ_{CO} can be explained in the same manner. Changing θ_{CO} from near-saturation monolayer coverage at 85 K to the low coverage obtained by heating this layer to 190 K causes a measured (total) shift of 14 cm^{-1} because changes in the chemical shift dominate over changes in dipolar-coupling shift as θ_{CO} decreases on the surface.

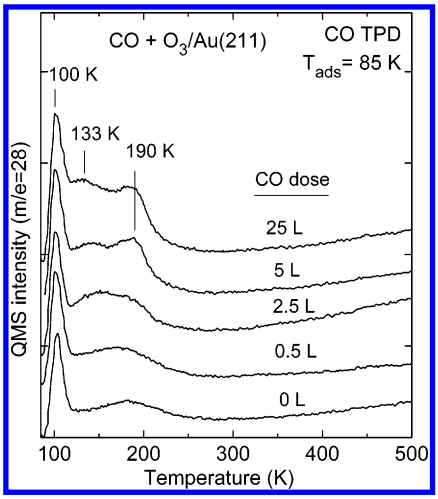

Figure 6. CO TPD curves obtained after exposing CO on an oxygen-precovered surface produced by a 100 langmuir O_3 exposure on the Au(211) surface at 85 K to create a saturation coverage of O adatoms. CO TPD peaks at 133 and 190 K indicate that some CO is reversibly adsorbed on the Au(211) after large CO doses.

Jugnet et al.[45] investigated CO adsorption on a Au(110) single crystal at CO pressures in the range of 0.1−100 torr by polarized IRAS. They observed only one ν_{CO} band at 2110 cm^{-1} with an intensity that depended on the CO pressure. In IRAS studies of CO adsorption on a stepped Au(332) surface at 92 K, Ruggiero and Hollins[25,26] found a single band at 2124 cm^{-1} that shifted 14 cm^{-1} to lower energy with increasing coverage. They measured a full width at half-maximum (fwhm) of 16 cm^{-1} for this band on Au(332) at 92 K under a dynamic pressure of 10^{-5} mbar CO and suggested that this band was composed of at least three vibrational components. We obtained a fwhm between 8 and 10 cm^{-1} with various exposures and 6−9 cm^{-1} after annealing. Therefore, the IR bands in our results appear to be composed of a single component, and CO bonding appears to be similar whether on step or terrace sites.

The change in chemical shift of ν_{CO} with coverage on Au(211) can be explained by the population of different sites as the coverage increases. CO adsorbs at step sites on Au(211) at low coverage, and so the appearance of ν_{CO} at higher wavenumbers for lower θ_{CO} can be attributed to CO adsorbed at step sites. Lower ν_{CO} values correspond to CO adsorbed at terrace sites. Even though CO binds more strongly at step sites, Au atoms at steps are undercoordinated, and this leads to higher ν_{CO} energies for CO adsorbed at these sites. Ruggiero and Hollins[25,26] explained their ν_{CO} shifts on Au(332) in this way rather than using chemical shift effects.

CO Titration of Preadsorbed Oxygen Adatoms on Au(211). Oxygen adatoms were created using ozone exposures (100 langmuir) on the Au(211) surface at 85 K (and also after annealing this surface to 300 K, not shown), and then the surface was given various CO exposures. As shown in Figure 6, CO TPD curves after small CO exposures (≤0.5 langmuir) are quite similar; however, additional peaks at 130 and 190 K were seen after higher CO doses (≥2.5 langmuir). These peaks at 130 and 190 K resemble those from CO desorption from the clean Au(211) surface as described in the previous section. Apparently,

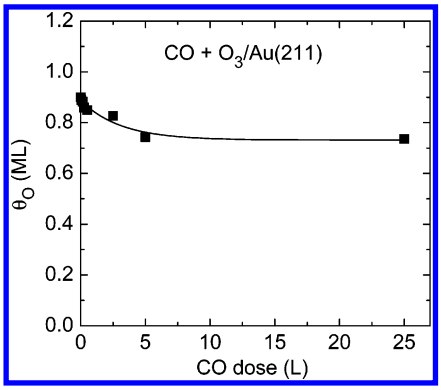

Figure 7. Plot of the coverage of oxygen left at the Au(211) surface following the CO exposures reported in Figure 6 and heating during subsequent TPD. The oxygen coverage was determined by the O_2 TPD peak areas obtained simultaneously in these experiments. The amount of oxygen at the Au(211) surface at 85 K was initially reduced efficiently by small CO doses, indicating a fast CO oxidation reaction transient, but then some oxygen that is much less reactive remains on the surface.

CO reacts with preadsorbed oxygen on the surface during CO dosing, even at this low temperature. IRAS spectra (not shown here) consistently show that very little adsorbed CO is present on the surface after exposing CO on the O-precovered Au(211) surface at 85 K. For large CO exposures, a small amount of CO can adsorb on the surface after reacting away accessible oxygen adatoms at 85 K. Figure 7 gives the amount of unreacted oxygen left on the surface following CO dosing as calculated from the O_2 TPD spectra that were obtained following these CO exposures on the Au(211) surface at 85 K. The oxygen coverage was reduced efficiently by small doses of CO, which demonstrates a fast rate for the CO oxidation reaction even at 85 K. The CO oxidation rate slowed during longer CO exposures, apparently due to the presence of a less reactive form of oxygen at the surface (perhaps a less accessible form of oxygen atoms such as incorporated or subsurface oxygen). Finally, we note that the bottom CO TPD curve in Figure 6, obtained without CO dosing, may arise from a cracking fraction from CO_2 desorption from adsorbed CO_2 that is found following large O_3 doses at low temperatures.

It was expected that Au(211) would exhibit quite a different reactivity than the flat Au(111) surface based on theoretical calculations.[36] Liu et al.[37] calculated using DFT that the CO adsorption energy on Au(211) would be 24.9 kcal mol^{-1} at 1/6 ML, which is 6 times larger than that from the Au(111) surface. Our results show a much smaller value for the CO adsorption energy compared to these DFT calculations, indicating that further refinement is needed in the calculations. However, with respect to CO adsorption, the calculated results of Mavrikakis et al.[36] are close to our experimental values. Overall, we find that the transient CO oxidation reaction probed in these CO titration experiments on the Au(211) surface does not appear to be significantly different from that on the flat Au(111) surface. Also, as we have reported in another paper,[20] the Au(211) surface does not dissociate O_2 at pressures up to 1 atm, and this is contrary to predictions from DFT calculations. Overall, from our experimental results, we conclude that it is unlikely that simply the presence of Au(211) planes (or other unstrained step sites) could be responsible for the high catalytic activity of CO oxidation on oxide-supported gold nanoparticles.

Conclusion

CO adsorption was investigated on the Au(211) stepped surface by using primarily TPD and IRAS. CO adsorbed onto the Au(211) surface at 85 K under UHV conditions, initially rapidly to populate step sites and then more slowly to fill up the terraces. A distinct peak in CO TPD was observed that was attributed to CO adsorbed at step sites. The corresponding CO desorption energy E_d was estimated to be 12 kcal mol^{-1}, indicating weak molecular chemisorption. At terrace sites, we estimated that $E_d = 6.5-9$ kcal mol^{-1}. The energy of the ν_{CO} band observed in IRAS indicates that CO adsorption occurs at atop sites under all conditions. The ν_{CO} band undergoes a red shift from 2112 to 2126 cm^{-1} with increasing CO coverage.

We find little difference between the CO chemisorption properties of the Au(211) surface, which can be described as 3(111) $\times$ (100) in microfacet notation, and other Au crystal planes or stepped surfaces, although it is significantly more reactive than the least-reactive Au(111) surface. Recent theoretical calculations that find that CO adsorbs much more strongly ($\sim 6\times$) on this stepped surface than on Au(111) are in error and need further refinement. Furthermore, based on our experimental results, we conclude that facets of bulklike Au(211) stepped surfaces that may be present on Au nanoparticles are unlikely to provide the reactive sites that are responsible for the remarkable properties reported for catalysts comprised of small Au nanoparticles on metal oxide supports.

Acknowledgment. This work was supported by the Department of Energy, Office of Basic Energy Sciences, Chemical Sciences Division.

References and Notes

(1) Haruta, M.; Kobayashi, T.; Sano, H.; Yamada, N. *Chem. Lett.* **1987**, *2*, 405.
(2) Haruta, M.; Yamada, N.; Kobayashi, T.; Iijima, S. *J. Catal.* **1989**, *115*, 301.
(3) Haruta, M.; Tsubota, S.; Kobayashi, T.; Kageyama, H.; Genet, M. J.; Delmon, B. *J. Catal.* **1993**, *144*, 175.
(4) Gardner, S. D.; Hoflund, G. B.; Upchurch, B. T.; Schryer, D. R.; Kielin, E. J.; Schryer, J. *J. Catal.* **1991**, *129*, 114.
(5) Knell, A.; Barnickel, P.; Baiker, A.; Wokaun, A. *J. Catal.* **1992**, *137*, 306.
(6) Cunningham, D.; Tsubota, S.; Kamijo, N.; Haruta, M. *Res. Chem. Intermed.* **1993**, *19*, 1.
(7) Lin, S. D.; Bollinger, M.; Vannice, M. A. *Catal. Lett.* **1993**, *17*, 245.
(8) Tanielyan, S. K.; Augustine, R. L. *Appl. Catal., A* **1992**, *85*, 73.
(9) Bollinger, M. A.; Vannice, M. A. *Appl. Catal., B* **1996**, *8*, 417.
(10) Liu, Z. M.; Vannice, M. A. *Catal. Lett.* **1997**, *43*, 51.
(11) Guczi, L.; Horvath, D.; Paszti, Z.; Toth, L.; Horvath, Z. E.; Karacs, A.; Peto, G. *J. Phys. Chem. B* **2000**, *104*, 3183.
(12) Boccuzzi, F.; Chiorino, A. *J. Phys. Chem. B* **2000**, *104*, 5414.
(13) Jia, J. F.; Kondo, J. N.; Domen, K.; Tamaru, K. *J. Phys. Chem. B* **2001**, *105*, 3017.
(14) Iizuka, Y.; Tode, T.; Takao, T.; Yatsu, K.; Takeuchi, T.; Tsubota, S.; Haruta, M. *J. Catal.* **1999**, *187*, 50.
(15) Schubert, M. M.; Hackenberg, S.; van Veen, A. C.; Muhler, M.; Plzak, V.; Behm, R. J. *J. Catal.* **2001**, *197*, 113.
(16) Grisel, R. J. H.; Nieuwenhuys, B. E. *J. Catal.* **2001**, *199*, 48.
(17) Kolmakov, A.; Goodman, D. W. *Surf. Sci.* **2001**, *490*, L597.
(18) Sault, A. G.; Madix, R. J.; Campbell, C. T. *Surf. Sci.* **1986**, *169*, 347.
(19) Outka, D. A.; Madix, R. J. *Surf. Sci.* **1987**, *179*, 351.
(20) Kim, J.; Samano, E.; Koel, B. E. *Surf. Sci.*, in press.
(21) McElhiney, G.; Pritchard, J. *Surf. Sci.* **1976**, *60*, 397.
(22) Lazaga, M. A.; Wickham, D. T.; Parker, D. H.; Kastanas, G. N.; Koel, B. E. In *Catalytic Selective Oxidation*; ACS Symposium Series 523; Hightower, J. W., Oyama, S. T., Eds.; American Chemical Society: Washington, DC, 1993; p 90.
(23) Sandell, A.; Bennich, P.; Nilsson, A.; Hernnas, B.; Bjorneholm, O.; Martensson, N. *Surf. Sci.* **1994**, *310*, 16.
(24) Gottfried, J. M.; Schmidt, K. J.; Schroeder, S. L. M.; Christmann, K. *Surf. Sci.* **2003**, *536*, 206.
(25) Ruggiero, C.; Hollins, P. *J. Chem. Soc., Faraday Trans.* **1996**, *92*, 4829.
(26) Ruggiero, C.; Hollins, P. *Surf. Sci.* **1997**, *377*, 583.

(27) Skelton, D. C.; Tobin, R. G.; Lambert, D. K.; DiMaggio, C. L.; Fisher, G. B. *J. Phys. Chem. B* **1999**, *103*, 964.
(28) Gleich, B.; Ruff, M.; Behm, R. J. *Surf. Sci.* **1997**, *386*, 48.
(29) Ruff, M.; Frey, S.; Gleich, B.; Behm, R. J. *Appl. Phys. A: Mater. Sci. Process.* **1998**, *66*, S513.
(30) Haruta, M. *CATTECH* **2002**, *6*, 102.
(31) Boccuzzi, F.; Chiorino, A.; Manzoli, M.; Lu, P.; Akita, T.; Ichikawa, S.; Haruta, M. *J. Catal.* **2001**, *202*, 256.
(32) Valden, M.; Pak, S.; Lai, X.; Goodman, D. W. *Catal. Lett.* **1998**, *56*, 7.
(33) Valden, M.; Lai, X.; Goodman, D. W. *Science* **1998**, *281*, 1647.
(34) Hakkinen, H.; Landman, U. *J. Am. Chem. Soc.* **2001**, *123*, 9704.
(35) Socaciu, L. D.; Hagen, J.; Bernhardt, T. M.; Woste, L.; Heiz, U.; Hakkinen, H.; Landman, U. *J. Am. Chem. Soc.* **2003**, *125*, 10437.
(36) Mavrikakis, M.; Stoltze, P.; Norskov, J. K. *Catal. Lett.* **2000**, *64*, 101.
(37) Liu, Z. P.; Hu, P.; Alavi, A. *J. Am. Chem. Soc.* **2002**, *124*, 14770.
(38) Wang, J.; Koel, B. E. *J. Phys. Chem. A* **1998**, *102*, 8573.
(39) Saliba, N.; Parker, D. H.; Koel, B. E. *Surf. Sci.* **1998**, *410*, 270.
(40) Bönicke, I.; Kirstein, W.; Spinzig, S.; Thieme, F. *Surf. Sci.* **1994**, *313*, 231.
(41) Collins, D. M.; Spicer, W. E. *Surf. Sci.* **1977**, *69*, 85.
(42) Dumas, P.; Tobin, R. G.; Richards, P. L. *Surf. Sci.* **1986**, *171*, 555.
(43) Dumas, P.; Tobin, R. G.; Richards, P. L. *J. Electron Spectrosc. Relat. Phenom.* **1986**, *39*, 183.
(44) France, J.; Hollins, P. *J. Electron Spectrosc. Relat. Phenom.* **1993**, *64*−*65*, 251.
(45) Jugnet, Y.; Aires, F.; Deranlot, C.; Piccolo, L.; Bertolini, J. C. *Surf. Sci.* **2002**, *521*, L639.